

UCSF

UC San Francisco Previously Published Works

Title

Synthesis and evaluation of tetrahydropyrazolopyridine inhibitors of anion exchange protein SLC26A4 (pendrin).

Permalink

<https://escholarship.org/uc/item/2q12s352>

Journal

Bioorganic & medicinal chemistry letters, 29(16)

ISSN

0960-894X

Authors

Zhu, Jie S
Lu, Julia Y
Tan, Joseph-Anthony
[et al.](#)

Publication Date

2019-08-01

DOI

10.1016/j.bmcl.2019.07.003

Peer reviewed



Published in final edited form as:

Bioorg Med Chem Lett. 2019 August 15; 29(16): 2119–2123. doi:10.1016/j.bmcl.2019.07.003.

Synthesis and evaluation of tetrahydropyrazolopyridine inhibitors of anion exchange protein SLC26A4 (pendrin)

Jie S. Zhu^a, Julia Y. Lu^a, Joseph-Anthony Tan^b, Amber A. Rivera^b, Puay-Wah Phuan^b, Marina E. Shatskikh^a, Jung-Ho Son^a, Peter M. Haggie^b, Alan S. Verkman^b, Mark J. Kurth^{a,*}

^aDepartment of Chemistry, University of California, Davis, CA 95616, United States

^bDepartments of Medicine & Physiology, University of California, San Francisco, CA 94143, United States

Abstract

Pendrin is a transmembrane chloride/anion antiporter that is strongly upregulated in the airways in rhinoviral infection, asthma, cystic fibrosis and chronic rhinosinusitis. Based on its role in the regulation of airway surface liquid depth, pendrin inhibitors have potential indications for treatment of inflammatory airways diseases. Here, a completely regioselective route to tetrahydropyrazolopyridine pendrin inhibitors based on 1,3-diketone and substituted hydrazine condensation was developed. Structure-activity relationships at the tetrahydropyridyl nitrogen were investigated using a focused library, establishing the privileged nature of *N*-phenyl ureas and improving inhibitor potency by greater than 2-fold.

Keywords

Pendrin; SLC26A4; Anion transporter; Pyrazole; Regioselectivity

1. Introduction

Pendrin (PDS) is a 780 amino acid sodium-independent chloride/ anion antiporter containing twelve putative transmembrane spanning domains and cytoplasmic amino and carboxy-termini.¹ The PDS gene (*SLC26A4*) was identified by positional cloning in subjects with the autosomal recessive disorder Pendred syndrome, which is characterized by hearing impairment and thyroid goiter.² Functional studies show that PDS mediates electroneutral exchange of Cl⁻ with various anions including I⁻, HCO₃⁻, OH⁻, and SCN⁻ at the apical membrane of epithelial cells in the inner ear, thyroid, kidney, airways, and adrenal gland.^{1,3–8} PDS upregulation is observed in the airways of humans with rhinovirus infection, asthma, cystic fibrosis and chronic rhinosinusitis, in rodent models of inflammatory pulmonary disease including asthma, infection, and toxin exposure, and in airway epithelial cultures after exposure to inflammatory cytokines.^{9–19} PDS knockout reduces pathology in various mouse models of inflammatory lung diseases.^{15,20} The mechanism of PDS

*Corresponding author. mjkurth@ucdavis.edu (M.J. Kurth).

Appendix A. Supplementary data

Supplementary data to this article can be found online at <https://doi.org/10.1016/j.bmcl.2019.07.003>

involvement in pulmonary inflammation is thought to involve regulation of airway surface liquid (ASL) volume. Small molecule PDS inhibitors increase airway hydration in cytokine stimulated human airway epithelial cultures.²¹ Together, these studies support the therapeutic utility of PDS inhibitors for lung diseases including asthma and cystic fibrosis.^{22,23}

Prior screening of 36,000 synthetic, drug-like small molecules identified several chemical classes of PDS inhibitors containing a tetrahydro-1*H*-pyrazolo[4,3-*c*]pyridine (TPP) core, with the most potent compound having an IC₅₀ of ~ 7 μM for both human and murine PDS (Fig 1A).^{21,24} Analysis of commercially available TPP pendrin inhibitor analogs revealed minimal opportunities for modification of the pyrazole nitrogen or ether oxygen.²¹ While substitutions at the tetrahydropyridyl nitrogen were relatively underexplored in the commercial library, the sulfonamide moiety – one of the most privileged functional groups in drug discovery²⁵ – was prevalent in PDS and *SLC26A3* inhibitors discovered by high-throughput screening (Fig 1B).^{21,26} We reasoned that developing a versatile route to TPP compounds would be valuable because chemical synthesis affords us the opportunity to generate a focused library at the tetrahydropyridyl nitrogen. Herein, we report the development of a completely regioselective route to the TPP core and structural analogs to further investigate structure–activity relationships for this class of compounds.

Work began by resynthesizing the original active compound (**1**). However, controlling the position of the *N*-methyl group was a major challenge due to regioselectivity issues associated with pyrazole synthesis.²⁷ Indeed, it is known that pyrazoles do not undergo selective *N*-alkylations and the reaction of *N*-substituted hydrazine with unsymmetrical 1,3-diketones is also not regioselective. Despite these challenges, the Knorr pyrazole synthesis remains one of the most robust and reliable methods for accessing these nitrogen heterocycles.²⁷ In order to address this regioselectivity problem, we took advantage of the benzylic CH₂–O moiety in the lead compound (Scheme 1). This moiety allowed us to attempt the Knorr pyrazole synthesis using an 1,3-diketone with an electron withdrawing group attached (**10**). Theoretically, the presence of the electron withdrawing group should activate the α- carbonyl, allowing selective pyrazole formation to occur.

The synthesis of **1** (Scheme 2) began with a Stork enamine synthesis between *N*-Boc piperidin-4-one and ethyl 2-chloro-2-oxoacetate. Hydrolysis of **13** using a biphasic system of DCM and aqueous HCl gave the ester-containing 1,3-diketone **10** in 85% yield over 3 steps at 25 g scale. Next, methylhydrazine was refluxed with **10** to deliver pyrazole **7** as the only regioisomer in 52% yield. Note, the reaction can also be stopped after just one day of reflux, but the yield of **7** decreases to 33%. Increasing the reaction time to three days did not give a higher yield of **7**. Routine purification of pyrazole **7** was straightforward because the undesired regioisomer was not formed/detected throughout the course of the reaction. This reaction was repeated on large scale and the structure of **7** was confirmed using X-ray crystallography (Scheme 3). Subsequent reduction of **7** using LiBH₄ gave the corresponding alcohol in 66% yield. Alcohol **6** was converted to bromide **14** in 84% yield using an Appel reaction.²⁸ It should be noted that NBS could be substituted completely by Br₂ with little impact on the yield of the Appel reaction. Reaction of 3-fluorophenol with **14** under basic conditions gave the targeted ether in 90% yield. The Boc group of **15** was more resilient than

expected, as deprotection using varying concentrations of HCl ranging from 1 to 6 M was ineffective in both methanol and dioxane. Boc deprotection was finally accomplished using TFA in DCM, followed by a basic work up to give amine **16**. Reaction of **16** with 4-chlorophenyl isocyanate gave the lead compound **1** in 77% yield over the last two steps. The synthesized **1** had a similar potency compared to commercial **1** (Figure 2).

As previously described, a functional cell-based assay of PDS-mediated Cl^-/I^- exchange was used to measure the PDS inhibition activity of TPP analogs.^{21,24} In brief, Fischer rat thyroid cells stably expressing murine PDS and a halide-sensitive fluorescent protein (EYFP-H148Q/I152L/F46L) were used. PDS activity was determined from the kinetics of fluorescence decrease in response to addition of an I^- containing solution to cells, with inhibitors reducing the rate of Cl^-/I^- exchange and hence the rate of reduction in fluorescence.

A small set of ether analogs were synthesized to address the effect of fluorine substitution (Table 1). These minor modifications improved PDS inhibition activity compared to compound **1**. Analogs **17** and **18** inhibited PDS with IC_{50} of 4.6 and 3.3 μM , while 3,5-difluoro-substituted **19** resulted in an IC_{50} of 3.1 μM . Ester analog **20** and carboxylic acid analog **21** both had minimal PDS inhibition activity.

Moving forward, the effect of substitution at the tetrahydropyridine nitrogen was investigated (see Fig 1A). Although previous high-throughput screening revealed that sulfonamides were common structural features among hit compounds, minimal inhibition activity was observed when sulfonamides were introduced into the TPP scaffold even when the 4-chlorophenyl moiety was preserved (Table 2).

Similarly, attempts to incorporate sulfur into the molecule *via* thioureas were not successful at increasing PDS inhibition activity. This series of analogs gave insights into the privileged nature of the *N*-phenyl urea, as both alkyl and acylated ureas performed poorly.

In summary, we developed a completely regioselective route to tetrahydropyrazolopyridines and synthesized a focused library of analogs with substitution at the tetrahydropyridyl nitrogen. This chemistry allowed us to further investigate the structure–activity relationship of this class of PDS inhibitors. Introduction of an additional fluorine atom significantly improved the IC_{50} from $\sim 7 \mu\text{M}$ to $\sim 3 \mu\text{M}$. Although the sulfur atom was well-represented in other classes of SLC26 inhibitors, sulfur analogs such as thioureas, sulfonamides, and sulfuric diamide were not useful for PDS inhibition activity. Indeed, throughout the course of these studies, *N*-phenyl ureas were found to be highly privileged.

Supplementary Material

Refer to Web version on PubMed Central for supplementary material.

Acknowledgments

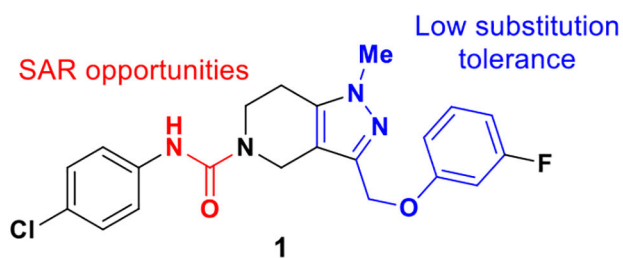
This work was supported by the National Institutes of Health (DK072517 and DK067003). J.S.Z. is supported by a fellowship from the UC Davis Tara K. Telford CF Fund, UC Davis Dissertation Year Fellowship, and R. Bryan Miller Graduate Fellowship. M.E.S. is supported by the UC Davis Provost's Undergraduate Fellowship.

References

1. Royaux IE, Suzuki K, Mori A, et al. Pendrin, the protein encoded by the Pendred syndrome gene (PDS), is an apical porter of iodide in the thyroid and is regulated by thyroglobulin in FRTL-5 cells. *Endocrinology*. 2000;141:839–845. [PubMed: 10650967]
2. Everett LA, Glaser B, Beck JC, et al. Pendred syndrome is caused by mutations in a putative sulphate transporter gene (PDS). *Nat Genet*. 1997;17:411–422. [PubMed: 9398842]
3. Pedemonte N, Caci E, Sondo E, et al. Thiocyanate transport in resting and IL-4-stimulated human bronchial epithelial cells: role of pendrin and anion channels. *J Immunol*. 2007;178:5144–5153. [PubMed: 17404297]
4. Royaux IE, Wall SM, Karniski LP, et al. Pendrin, encoded by the Pendred syndrome gene, resides in the apical region of renal intercalated cells and mediates bicarbonate secretion. *PNAS*. 2001;98:4221–4226. [PubMed: 11274445]
5. Scott DA, Karniski LP. Human pendrin expressed in *Xenopus laevis* oocytes mediates chloride/formate exchange. *Am J Physiol Cell Physiol*. 2000;278:C207–C211. [PubMed: 10644529]
6. Scott DA, Wang R, Kremann TM, Sheffield VC, Karniski LP. The Pendred syndrome gene encodes a chloride-iodide transport protein. *Nat Genet*. 1999;21:440. [PubMed: 10192399]
7. Shcheynikov N, Yang D, Wang Y, et al. The Slc26a4 transporter functions as an electroneutral Cl⁻/I⁻/HCO₃⁻ exchanger: role of Slc26a4 and Slc26a6 in I⁻ and HCO₃⁻ secretion and in regulation of CFTR in the parotid duct. *J Physiol*. 2008;586:3813–3824. [PubMed: 18565999]
8. Soleimani M, Greeley T, Petrovic S, et al. Pendrin: an apical Cl⁻/OH⁻/HCO₃⁻ exchanger in the kidney cortex. *Am J Physiol Renal Physiol*. 2001;280:F356–F364. [PubMed: 11208611]
9. Adams KM, Abraham V, Spielman D, et al. IL-17A Induces Pendrin Expression and Chloride-Bicarbonate Exchange in Human Bronchial Epithelial Cells. *PLoS ONE*. 2014;9:e103263. [PubMed: 25141009]
10. Clarke LA, Sousa L, Barreto C, Amaral MD. Changes in transcriptome of native nasal epithelium expressing F508del-CFTR and intersecting data from comparable studies. *Respir Res*. 2013;14:38. [PubMed: 23537407]
11. Fujita K, Morimoto Y, Endoh S, et al. Identification of potential biomarkers from gene expression profiles in rat lungs intratracheally instilled with C(60) fullerenes. *Toxicology*. 2010;274:34–41. [PubMed: 20471445]
12. Ishida A, Ohta N, Suzuki Y, et al. Expression of pendrin and periostin in allergic rhinitis and chronic rhinosinusitis. *Allergol Int*. 2012;61:589–595. [PubMed: 22918213]
13. Kuperman DA, Lewis CC, Woodruff PG, et al. Dissecting asthma using focused transgenic modeling and functional genomics. *J Allergy Clin Immunol*. 2005;116:305–311. [PubMed: 16083784]
14. Lewis CC, Yang JYH, Huang X, et al. Disease-specific gene expression profiling in multiple models of lung disease. *Am J Respir Crit Care Med*. 2008;177:376–387. [PubMed: 18029791]
15. Nakagami Y, Favoretto S Jr., Zhen G, Park S-W, Nguyenvu LT, Kuperman DA, Dolganov GM, Huang X, Boushey HA, Avila PC, Erle DJ. The epithelial anion transporter pendrin is induced by allergy and rhinovirus infection, regulates airway surface liquid, and increases airway reactivity and inflammation in an asthma model. *Am J Immunol*. 2008;181:2203–2210.
16. Nakao I, Kanaji S, Ohta S, et al. Identification of pendrin as a common mediator for mucus production in bronchial asthma and chronic obstructive pulmonary disease. *J Immunol*. 2008;180:6262–6269. [PubMed: 18424749]
17. Oh J-H, Yang M-J, Heo J-D, et al. Inflammatory response in rat lungs with recurrent exposure to welding fumes: a transcriptomic approach. *Toxicol Ind Health*. 2011;28:203–215. [PubMed: 21730038]
18. Seshadri S, Lu X, Purkey MR, et al. Increased expression of the epithelial anion transporter pendrin/SLC26A4 in nasal polyps of patients with chronic rhinosinusitis. *J Allergy Clin Immunol*. 2015;136(1548–1558):e7.
19. Yick CY, Zwinderman AH, Kunst PW, et al. Transcriptome sequencing (RNA-Seq) of human endobronchial biopsies: asthma versus controls. *Eur Respir J*. 2013;42:662–670. [PubMed: 23314903]

20. Scanlon KM, Gau Y, Zhu J, et al. Epithelial anion transporter pendrin contributes to inflammatory lung pathology in mouse models of *Bordetella pertussis* infection. *Infect Immun*. 2014;82:4212–4221. [PubMed: 25069981]
21. Haggie PM, Phuan PW, Tan JA, Zlock L, Finkbeiner WE, Verkman AS. Inhibitors of pendrin anion exchange identified in a small molecule screen increase airway surface liquid volume in cystic fibrosis. *FASEB J*. 2016;30:2187–2197. [PubMed: 26932931]
22. Li H, Salomon JJ, Sheppard DN, Mall MA, Galiotta LJ. Bypassing CFTR dysfunction in cystic fibrosis with alternative pathways for anion transport. *Curr Opin Pharmacol*. 2017;34:91–97. [PubMed: 29065356]
23. Sala-Rabanal M, Yurtsever Z, Berry KN, Brett TJ. Novel Roles for Chloride Channels, Exchangers, and Regulators in Chronic Inflammatory Airway Diseases. *Mediators Inflamm*. 2015;2015:13.
24. Cil O, Haggie PM, Phuan P-W, Tan J-A, Verkman AS. Small-Molecule Inhibitors of Pendrin Potentiate the Diuretic Action of Furosemide. *J Am Soc Nephrol*. 2016;27:3706–3714. [PubMed: 27153921]
25. Scott KA, Njardarson JT. Analysis of US FDA-Approved Drugs Containing Sulfur Atoms. *Top Curr Chem*. 2018;376:5.
26. Haggie PM, Cil O, Lee S, et al. SLC26A3 inhibitor identified in small molecule screen blocks colonic fluid absorption and reduces constipation. *JCI Insight*. 2018;3.
27. Karrouchi K, Radi S, Ramli Y, et al. Synthesis and Pharmacological Activities of Pyrazole Derivatives: A Review. *Molecules*. 2018;23.
28. Appel R Tertiary Phosphane/Tetrachloromethane, a Versatile Reagent for Chlorination, Dehydration, and P—N Linkage. *Angew Chem Int Ed Engl*. 1975;14:801–811.

A) TPP pendrin inhibitor from high-throughput screening



B) Sulfur-containing targets from high-throughput screening

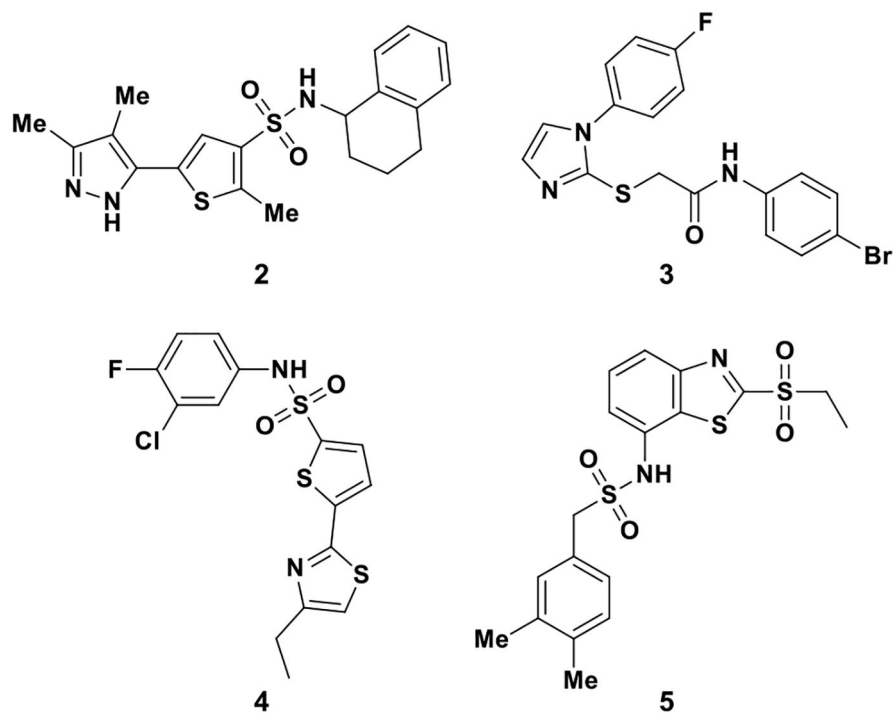


Fig 1.
Previously identified inhibitors of *SLC26A4* and *SLC26A3*.

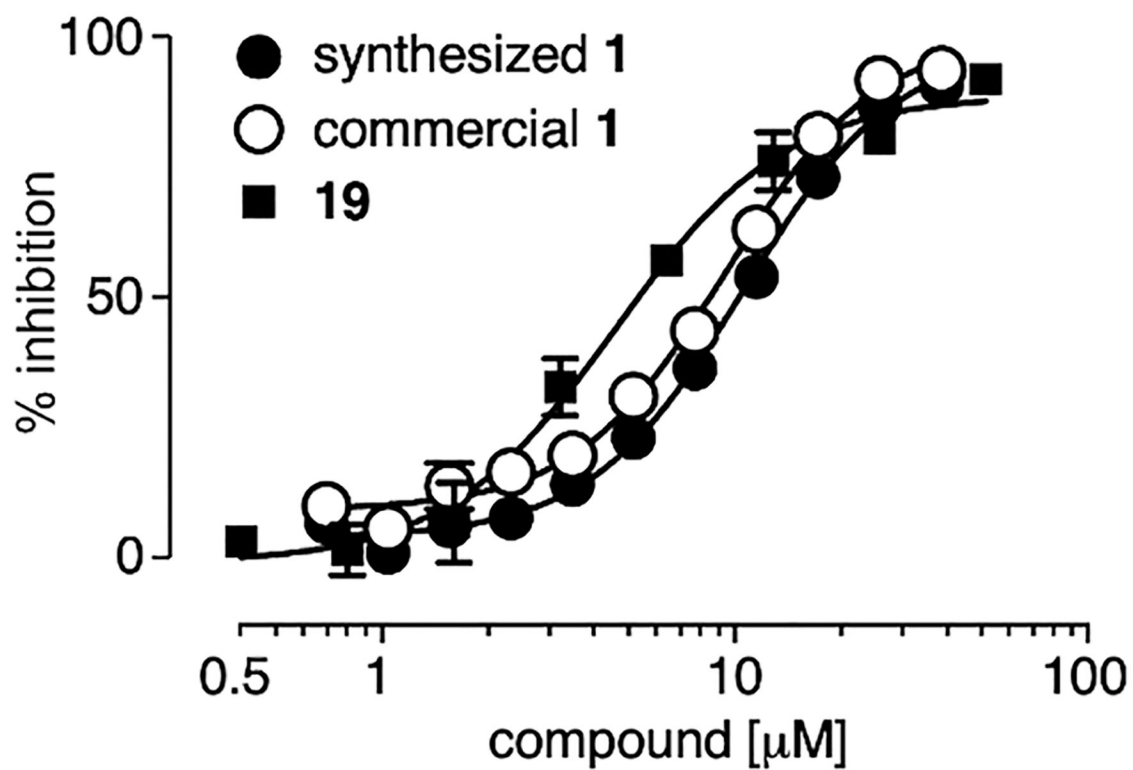
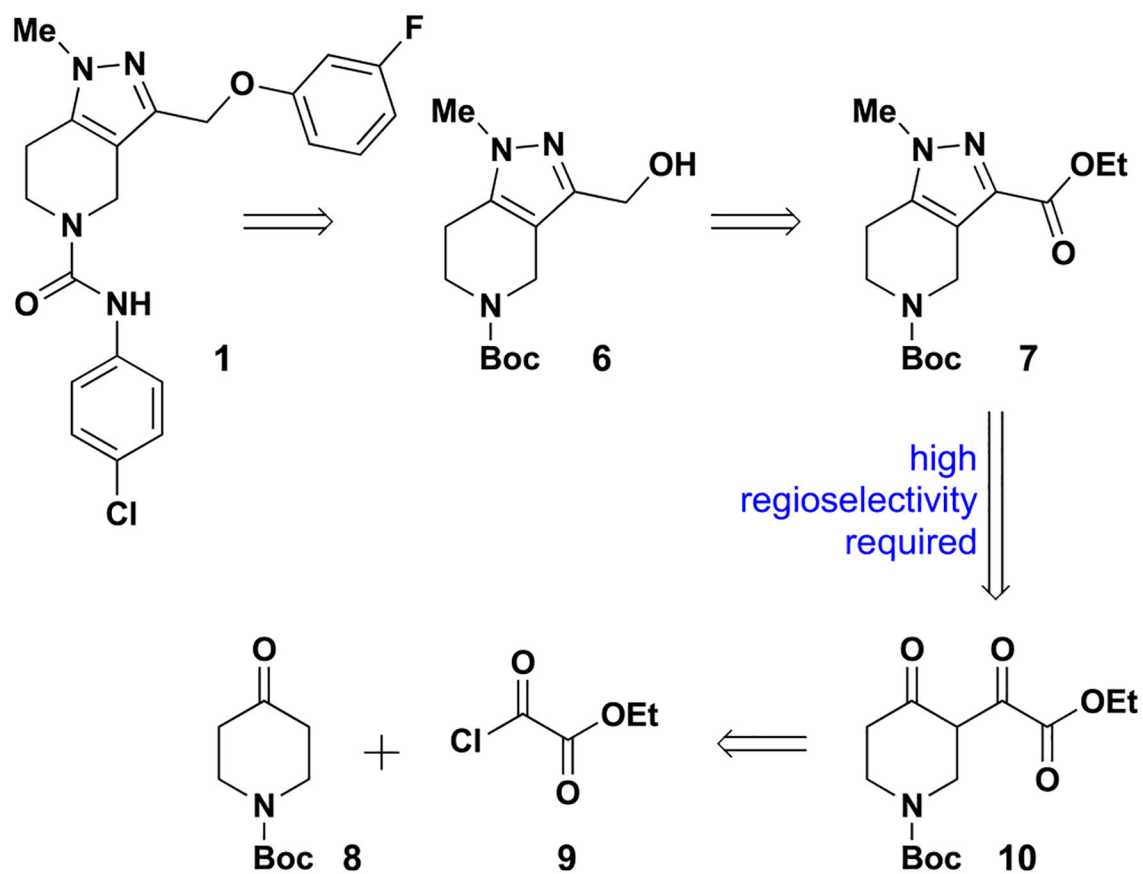
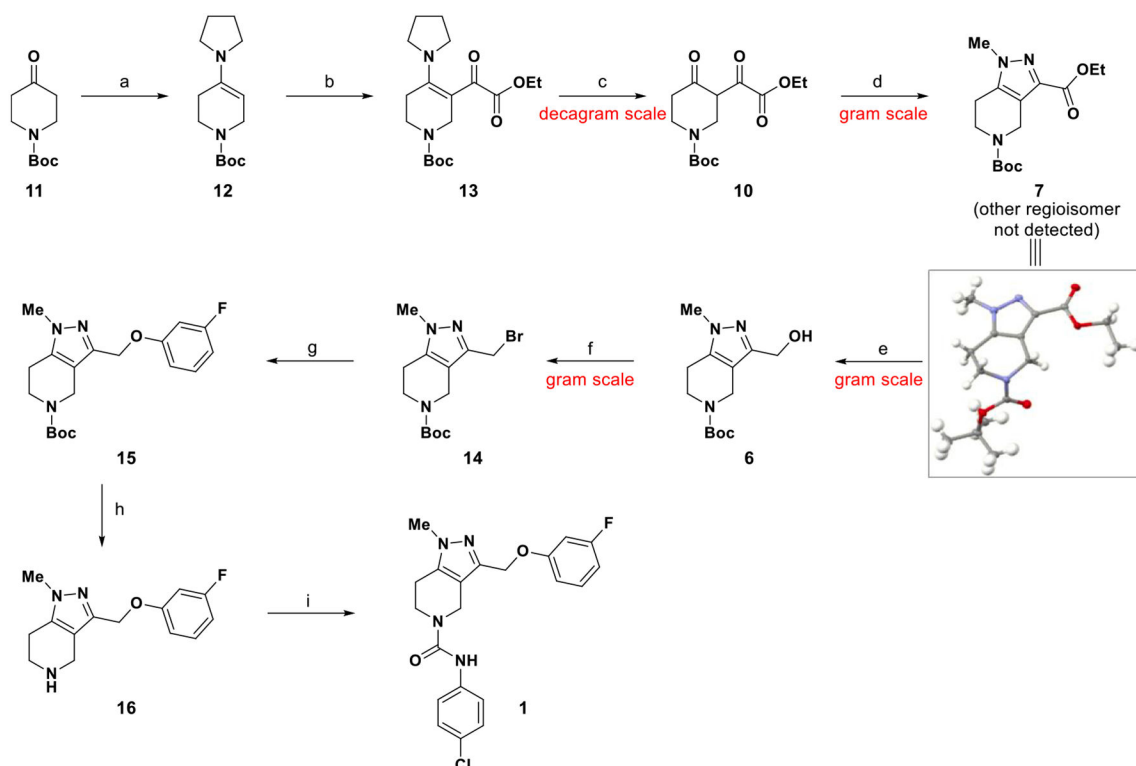


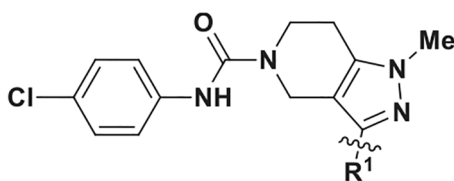
Fig 2.
Concentration-dependence for inhibition of pendrin anion exchange by synthesized and commercial **1**, and by **19**.



Scheme 1.
Retrosynthetic analysis.



Scheme 2.
Regioselective synthesis of the lead compound.



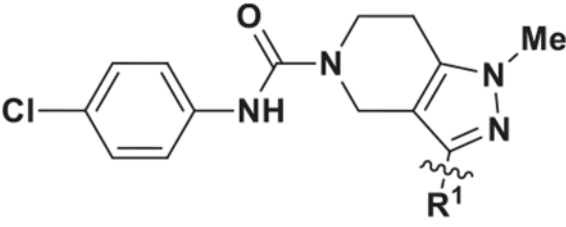
Comp.	R ¹	PDS IC ₅₀
1		6.6 μM
17		4.6 μM
19		3.1 μM
18		3.3 μM
20		>10 μM
21		>10 μM

Scheme 3.

Regioselective synthesis of the lead compound. Reagents and conditions: (a) pyrrolidine, toluene, Dean-Stark, reflux; (b) ethyl chlorooxacetate, Et 3N, DCM, rt; (c) DCM, 1 M HCl, rt, 85% over 3 steps; (d) methylhydrazine, EtOH, reflux, 52%; (e) LiBH₄, Et₂O, reflux, 66%; (f) PPh₃, NBS, DCM, rt, 84%; (g) 3-fluorophenol, Cs₂CO₃, DMF, 90 °C, 90%; (h) TFA, DCM, rt; (i) 4-chlorophenyl isocyanate, DCM (anh), rt, 77% over 2 steps.

Table 1

Synthesized TPP with varying substitution at benzylic position and activity against PDS.



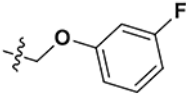
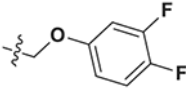
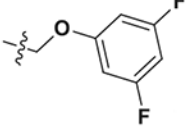
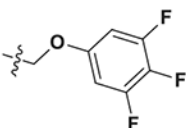
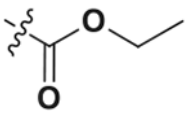
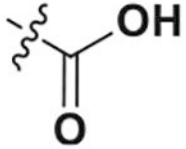
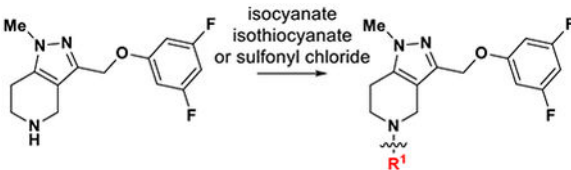
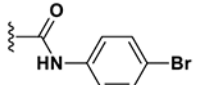
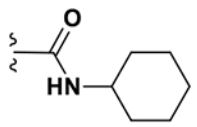
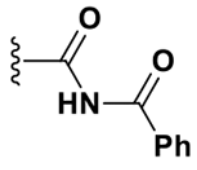
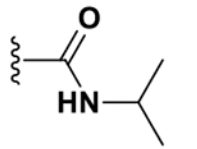
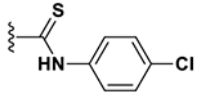
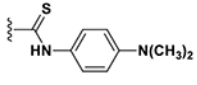
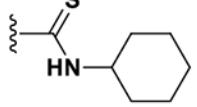
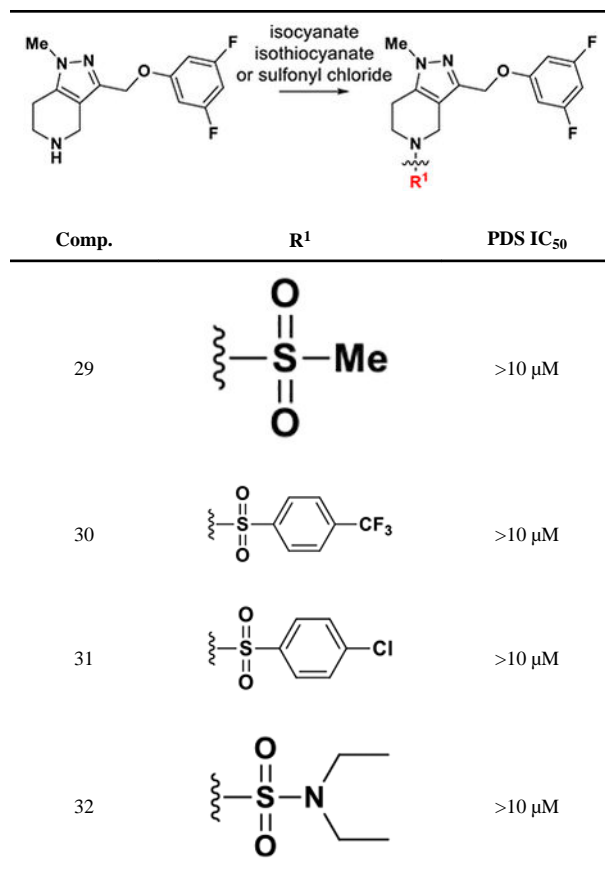
Comp.	R ¹	PDS IC ₅₀
1		6.6 μM
17		4.6 μM
19		3.1 μM
18		3.3 μM
20		>10 μM
21		>10 μM

Table 2

TPP with different substitution patterns at tetrahydropyridyl nitrogen and activity against PDS.



Comp.	R ¹	PDS IC ₅₀
22		3.3 μM
23		>10 μM
24		>10 μM
25		>10 μM
26		>10 μM
27		>10 μM
28		>10 μM



Author Manuscript

Author Manuscript

Author Manuscript

Author Manuscript